

# THE INTERNATIONAL JOURNAL OF SCIENCE & TECHNOLEDGE

## Segmentation of Gastroenterology Images Using Normalized Cuts

**T. Sudhalavanya**

M.E Applied Electronics, Final Year Student, Department of Electronics & Communication Engineering  
K.S. Rangasamy College of Technology, Tiruchengode, Tamil Nadu, India

**S. S. Thamilselvi**

Assistant Professor, Department of Electronics & Communication Engineering,  
K.S. Rangasamy College of Technology, Tiruchengode, Tamil Nadu, India

### **Abstract:**

*Gastroenterology imaging is an essential tool to detect gastrointestinal cancer in patients. This paper presents a novel method for the segmentation of gastroenterology images from two distinct imaging modalities and organs: chromoendoscopy (CH) and narrow-band imaging (NBI) from stomach and esophagus, respectively. The proposed method used various visual features individually and their combinations (edgemaps, creaseness, and color) in normalized cuts image segmentation framework to segment ground truth datasets of 142 CH and 224 NBI images. Experiments show that an integration of edgemaps and creaseness in normalized cuts gives the best segmentation performance resulting in high-quality segmentations of the gastroenterology images.*

### **1. Introduction**

Gastrointestinal cancer refers to malignant conditions of gastrointestinal tract (GI tract) including the esophagus, stomach, small intestine, large intestine. The symptoms relate to the organ affected and can include obstruction, abnormal bleeding or other associated problems.

Gastrointestinal cancer is diagnosed using microscopic analysis of histopathological colon samples. In such an examination, pathologists observe the colon samples under microscope to detect malignancy, and assign cancer grade depending upon the level of organizational changes they observe in tissues. But, the manual examination has a few limitations. First, it is subjective because quantitative measures such as cancer grades/stages mainly depend on the visual assessment of pathologists. Second, it has inter/ intra observer variation in grading. Such vulnerabilities in the manual process result in need of automatic colon cancer diagnostic techniques, which could provide second opinion to the pathologists in the short run and could serve as an independent trustworthy system for detection of cancer in the long run. Automatic detection of Gastrointestinal cancer has two major directions: segmentation and classification.

In segmentation, heterogeneous colon samples are segregated into homogenous regions based on spatial distribution of tissues in the images. Next, normal and malignant labels are assigned to the regions based on certain features. In the literature, several approaches exist for medical image segmentation such as pixel based, region based, and graph based. Pixel-based methods divide image pixels into different clusters based upon their colors using various approaches like watershed transform, clustering, adaptive segmentation, and thresholding. Region-based segmentation methodologies use similar approach, but they maintain connectivity between pixels of similar clusters. Well-known techniques of this category include splitting and merging and region growing. Graph-based techniques assumes image pixels as nodes of a graph, and weight between them as similarity between pixels. Segmentation then involves graph partitioning into subgraphs while minimizing cost functions. In classification, colon samples are divided into normal and malignant categories based upon certain features. Classification and segmentation may be followed by cancer grading step, in which quantitative cancer grades are assigned to the samples depending upon certain quantitative measures.

## 2. Methodology

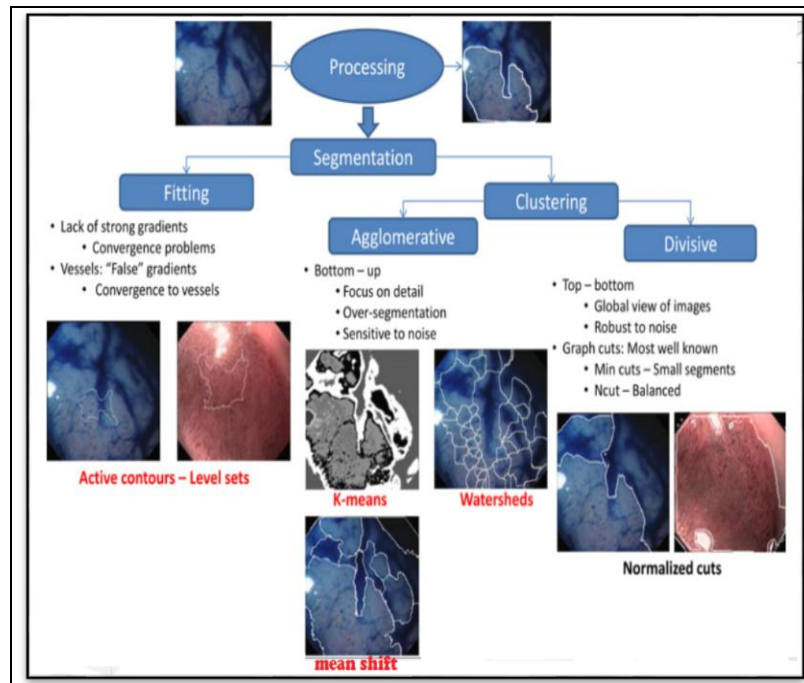


Figure 1: Segmentation using various methods. Ncut is the most relevant choice given its more global approach

### 2.1. Segmentation

Segmentation is divided into two main categories:

#### 2.1.1. Segmentation by Fitting:

The most well-known methods from this category are known as "active contours." These are dynamic contours that move toward the object boundaries. In these methods, a closed contour is initially selected that iteratively evolves to settle at these boundaries. These methods are divided into two main categories: parametric deformable models and geometric deformable models. Contours are used to measure dissimilarity between the pixels in an image

#### 2.1.2. Segmentation by Clustering:

In segmentation by clustering, all the pixels in an image are grouped together based on similarity in their visual characteristics such as brightness, texture, color, etc. There are two natural approaches to clustering: Agglomerative Clustering and Divisive Clustering. In agglomerative clustering, each pixel is initially regarded as an individual cluster. These clusters are recursively merged to yield various image regions. The merging criteria can vary with the nature of the applied segmentation scenarios. Some of the most common and widely used agglomerative clustering methods are K-means, watersheds, etc.

## 3. Materials

A GI tract consists of a number of organs: mouth, esophagus, stomach, small intestine, and large intestine. The anatomy and structure of various organs are responsible for different difficulties during a GI exam. Here two complementary GI organ images are taken by using complementary imaging modalities: chromoendoscopy (CH) for diagnosis of stomach cancer and NBI for diagnosis of esophagus. CH and NBI images exhibit different visual characteristics: the former uses the full visible spectrum of light for tissue illumination and benefits from enhancement achieved by dyes (e.g., methylene blue), improving the visibility of the gastric mucosa. The latter uses two small bands of the visible spectrum (e.g., blue and green), producing images which have a much poorer color resolution but rich visibility of the vasculature of the illuminated tissue. For our experiments, the procedures to obtain data are as follows.

### 3.1. CH Images

Chromoendoscopy involves topical application of various dyes during endoscopy which improves the visualisation of mucosal surfaces. The stains can be divided into three main classes: contrast, absorptive and reactive. Contrast stains, for example indigo carmine (IC), accumulate in the mucosal fissures thereby accentuating surface topology. In contrast, absorptive stains such as Lugol's iodine (LI), crystal violet and methylene blue (MB) are absorbed into components of the cellular structure in the mucosa. Differences in the uptake of these stains can therefore be used to elucidate different types of mucosa. There are two essential steps in

chromoendoscopy - firstly, removal of mucous which is then followed by dye application. This can be achieved by flushing the agent through the working channel using a spray catheter or even administering it as an oral solution before the endoscopic procedure. Once the mucous is cleared, the dye can then be applied. The volume, concentration and the dye contact time varies considerably.

### 3.2. NBI Images

The quest for a simpler technique which would obviate the complexity of chromoendoscopy led to the development of narrow band imaging (NBI). Standard white light endoscopy consists of 3 light waves: blue, green and red. The principles behind NBI technology are that the bandwidths of blue (440-460 nm) and green (540-560 nm) wave light are narrowed whilst the contribution of red wave light is totally negated out of the emitted light. This is achieved by a special filter which is electronically activated once the endoscopist presses a switch on the endoscope. The whole process takes less than 1s and is practical during any endoscopy procedure provided the system is equipped with NBI. The narrowed bandwidths of green and blue light lead to superficial penetration of the mucosa accentuating the microvasculature pattern as haemoglobin has a peak absorption spectrum towards both these wave lengths. The quality of the surface pit pattern morphology is also clearly enhanced by this technology.

## 4. Computer Vision for Gastroenterology

### 4.1. Introduction

In this chapter discuss the latest state-of-the-art in computer vision (CV) for diagnosis of abnormalities in the gastrointestinal (GI) tract. In this chapter was modularized according to the detection of the following abnormalities: Ulcer and bleeding detection, Polyp detection, abnormality detection and Diagnosis of cancer.

#### 4.1.1. Ulcer And Bleeding Detection

Hwang at al. [1] proposed an algorithm that they claimed to have used for detection of bleeding in wireless capsule endoscopy images. The authors did a manual selection of blood and non-blood pixels to train their respective probability models. For this method, it is important to know that there is a certain color range distinguishing blood pixels from non-blood pixels. However, most dark pixels representing blood can overlap with the dark pixels in non-blood pixels having no chrominance. The NCut clustering algorithm is used to train the probability models for blood and non blood pixels. The theoretical foundation of the paper is interesting and good results are obtained. However, the proposed methodology is not invariant to illumination changes in the images. Also, the model parameters are learned using the training dataset. The results obtained are therefore highly dependent on the training data. Another shortcoming is that the testing pool used in these experiments is quite small and an extended validation of the method needs to be carried out.

M. Mackiewicz et al. [2] chose a histogram based approach for the detection of bleeding. They claim that this is necessary for fast model adaptation which is easier using non-parametric methods contrary to Hwang's [1] method (where the model parameters are learned using training data). Their approach uses adaptive color histograms to track the moving background and bleeding color distributions over time in capsule endoscopy (CE) videos. It therefore addresses the problems of drastic changes in blood color distributions due to GI fluids and thus helps in detection of red lesions when the difference between their color distribution and background is large enough. In the second stage of the algorithm, they analyzed all candidate blood frames using Hue-Saturation-Intensity (HSI) and Local Binary Pattern (LBP) features. Results show that their method compares favourably with Suspected Blood Indicator (SBI) by Given Imaging. Since this method does not produce illumination invariant color features, it is not expected to discriminate between dark bleeding tissues and those that appear dark and are normal.

Li and Meng [3] proposed the idea of using a combination of chrominance moments and Local Binary Patterns (LBP) as the image features to discriminate between normal and abnormal regions. HSI color space was adopted for the desired experiments and hue and saturation components were used to achieve illumination invariance. The wireless capsule endoscopy (WCE) images were divided into a number of block based regions (Fig. 4.2) that were chosen for feature extraction. A Neural network classifier was used for the classification task. Although good results were obtained, this study needs a stronger validation as the training and test sets were allowed to be composed of image blocks from the same patient sequence due to the lack of adequate data for relevant statistical evaluation of the algorithm.

Li and Meng [4] proposed a novel approach for detection of ulcers in capsule endoscopy images. They used uniform LBP of curvelet transformed images as texture features to distinguish between normal regions in the images and ulcers. The proposed features capture multi-directional features and show robustness to illumination changes. Multilayer perceptrons and support vector machines were used as classifiers. Although the results obtained were very good, features were extracted from image blocks that were obtained by a grid based segmentation of capsule images. The rationale that the authors have adopted for this strategy is that for feature extraction from full images, some detailed micro image characteristics might be disregarded. The proposed method has been used for ulcer detection on large amount of data, however it was collected from only 5 patients. For an extensive testing of the proposed method, a dataset from more patients should be included in the study.

#### 4.1.2. Polyp Detection

Karkanis et al. [5] proposed a computer aided tumor detection method in endoscopic images using color wavelet features. These are based on covariance of second order textural feature over wavelet frames. The methodology has been applied to a rich dataset of color colonoscopy videos with very good overall performance achieved for the detection of polyps.

S. Hwang and M. Celebi [6] proposed a novel method for the detection of polyps. They used watershed segmentation using a novel initial marker selection method using Gabor Filters and K-means clustering. After a preliminary segmentation of the image, polyp candidates are identified assuming that they should be circular or elliptical. Curvature centres are calculated using the boundary of the polyp candidates where most of them should be located inside the polyp region. Good results for identification of polyps were obtained with a very high sensitivity but slightly lower specificity. The authors pointed out that the low specificity was due to the richness of texture exhibited by some non-polyp regions, which were classified by the algorithm as polyps.

A. Karargyris and N. Bourbakis [7] proposed a method to detect polyps in the bowel. They used Log-Gabor filters followed by SUSAN edge detector to do segmentation of capsule images. The algorithm runs around the boundary of the segmented part calculating the curvature at each point. For points having a certain curvature, the centres of curvature are detected. A cloud of curvature points inside the segmented image regions is found. A simple two-threshold sequential clustering is later used to cluster the curvature points. Starting from those cluster centers, active contours are used to expand the cluster on the gray level image to obtain the desired polyps. As in the previous method, the specificity of the algorithm is low and it is attributed to the regions having crisp texture while being a non-polyp. Rules based decision making in such cases to identify polyp candidates as done for SUSAN edge detection and curvature calculation could be manipulated to strongly effect specificity of the algorithm. These decisions are therefore expected to be data driven. Also, it is a synergistic approach and the use of both SUSAN edge detector and active contours significantly increases the complexity of the proposed methodology.

#### 4.1.3. Diagnosis of Cancer

C. Demir and Y. Demer [8] present a systematic survey of various methods that have been used for the design of computer assisted decision system for cancer diagnosis. Based on this survey, the authors have identified three important steps, which are usually involved in all such systems i.e., pre-processing, feature extraction and classification. They discuss various methods that have been used by different researchers for these tasks. This paper highlights an important issue in the area of automated diagnosis of cancer which is the lack of availability of data. Several research groups are working on this line of research however it is not possible to make a fair comparison of their performance achieved due to the lack of an open gold standard database. It is therefore essential to form a benchmark of datasets with the classification results backed by their biopsy reports.

M. Hafner et al. [9] make use of ring filters for feature extraction followed by classification using support vector machines (SVM). The ring filters are a combination Figure 4.5: An image representing Aberrant Crypt Foci in colonic images of isotropic band pass filters. The authors have pointed out that their fourier based features are among the best performing however they are slightly inferior as compared to the Dual-Tree Complex Wavelet Transform (DTCWT) and Local Binary Pattern (LBP) features. We suspect that this happens because contrary to the DTCWT, the ring filters are not capable of directional selectivity thus limiting their use in extracting certain texture characteristics. The authors also hinted that it would not be sensible to make a direct comparison between the performances reported by various authors in their papers as compared to their methods since the performance should be measured on the same datasets for being directly comparable.

A. Sousa et al. [10] made use of the adapted color histograms for classification of cancer in gastroenterology (GE) images. They did a survey on these images to conclude that the colors in GE images do not span the full spectrum of the color spaces. The richness of colors therefore lies in some particular regions in the color space. They introduced adapted color spaces to enhance color resolution in the space where the occurrence frequency of the colors is high and compromised on resolution where occurrence frequency was low. The proposed descriptor was combined with Local Binary Patterns to classify endoscopic images into three different classes: normal, pre-cancer and cancer. They obtained very good classification results. It is important to note that these are very specific histograms for which the validation was done on vital stained images. Other staining agents can lead to a different distribution of colors in the color space thus the histogram bins need to be recalculated by vector quantization of the color space. Texture features on the other hand are useful for classifying images from most of the imaging modalities.

## **5. Segmentation**

### *5.1. Description*

- The proposed methodology is applied to the scenario of segmentation of GE images from two complementary imaging modalities, CH and narrow-band imaging (NBI), from two different organs, i.e., stomach and esophagus, respectively.
- Model the boundaries of clinically relevant regions in GE images as creases in a topographic surface using multilocal creaseness features. These are used to construct undirected, weighted graphs of the images. Ncut is applied to these graphs for doing image segmentation. In this intervening contours are used to measure dissimilarity between the pixels in an image.
- The multiple image features including edgemaps, creaseness, and color features are used to enhance the segmentation performance, thus giving highquality image segmentations for the different imaging modalities.

### 5.2. Normalized Cuts

NCut is a graph-theoretic approach for solving the grouping problem in vision. It is a clustering-based segmentation approach in which an image is represented as a weighted, undirected graph whose nodes correspond to individual pixels and graph weights are based on affinity between the pixels.

Given a graph  $G = (V, E, W)$ , where  $V$  is the set of nodes and  $E$  is the set of edges connecting the nodes having weights given by a weight matrix  $W$ .

A pair of nodes  $u$  and  $v$  is connected by an edge weighted by  $w(u, v) = w(v, u) \geq 0$  to measure the similarity between them. The graph can be partitioned into two disjoint sets  $A$  and  $B = V - A$  by removing the edges joining the two parts. The degree of dissimilarity between the two sets can be computed as the total weight of the removed edges. This leads to the following mathematical formulation of a cut:

$$\text{Cut}(A, B) = \sum_{u \in A, v \in B} w(u, v)$$

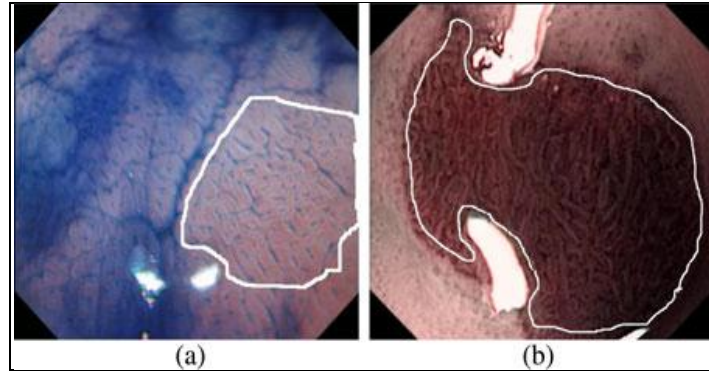


Figure 2: Manual annotation of clinically relevant regions in GE images.  
(a) CH image. (b) NBI image.

Minimum cuts criterion, however, favors grouping small sets of isolated nodes in the graph since the cut defined above does not incorporate any intragroup information, thus resulting in oversegmentation of the image. This motivates the formation of several modified graph partitioning methods including the NCut.

$$\text{NCut} = \frac{\text{cut}(A, B)}{\text{assoc}(A, V)} + \frac{\text{cut}(A, B)}{\text{assoc}(B, V)}$$

where  $\text{assoc}(A, V)$  denotes the total connection from nodes in  $A$  to all nodes in the graph and  $\text{assoc}(B, V)$  is similarly defined. Unlike the minimum criterion that has a bias toward cutting small sets of nodes, the NCut presents an unbiased criterion.

### 5.3. Visual Features for Affinity Calculation

NCut has the intrinsic ability to combine a set of features to calculate the affinity matrix to be used for images segmentation. In this section describe the particular features that selected for calculating this affinity matrix.

#### 5.3.1. Multiscale Edgmaps

Edge maps are one of the most important features for segmentation of an image. For calculating edgmaps, filters are employed. These are designed to detect the edges at different scales and different orientations. The odd-phased filters ( $F_o(\sigma)$ ) are first-order derivatives whereas even-phased filters ( $F_e(\sigma)$ ) are second-order derivatives, both smoothed with Gaussians specified by their standard deviations.

$$E(\sigma) = (I * F_o(\sigma))^2 + (I * F_e(\sigma))^2$$

$E(\sigma)$  is a function of scale of the filter. The filter responses are calculated using filters at different scales. The affinity from edgmaps is calculated using the following mapping:

$$D^{E*} = 1 - e^{-E*}$$

This mapping of filter energy ensures that the values of affinity range between 0 and 1, indicating no or high affinity, respectively.

#### 5.3.2. Multilocal Creaseness

Edges are one of the most common visual features for image segmentation. However, in imaging scenarios where the images have very rich texture content, extraction of edges can result in an enhancement of the local texture in the images. Therefore, when these features are used for applications such as image segmentation, an oversegmentation of images is a typical outcome which is undesirable in most cases. Creaseness features provide an intuitive solution to this problem and several measures of creaseness have the potential to serve the purpose. In this project uses the multilocal level set extrinsic curvature with enhancement by structure tensor (MLSEC-ST) operator to enhance the ridge and valley patterns in the images. MLSEC-ST has the potential to deal with the heavily jagged texture efficiently. The affinity is calculated using the following mapping:

$$D_{Cr} = 1 - e^{-(\lambda_1(x) - \lambda_2(x))^2}$$

Where  $\lambda_1(x) > \lambda_2(x) \geq 0$  are the eigenvalues of the structure tensor  $S(x)$ . creaseness features enhance the tissue boundaries significantly while suppressing the local texture of the regions in the images. These features are suitable for segmentation of tissue boundaries of GE images.

5.3.3 Color Features

In this project employe the  $L^*u^*v^*$  color space for extracting color features of the images. If  $c_u$  and  $c_v$  are colors of pixels  $u$  and  $v$ , respectively, the difference between the colors can be represented as

$$DCo = 1 - e^{-||c_u - c_v||^2}$$

5.4. Calculating Affinity from Visual Features

For generating the affinity matrix is need to calculate affinity measures between the sets of pixels in the images. In this implementation intervening contours framework is used for calculating affinity matrix. Fig. 3 illustrates the intuition behind this idea: left figure is an image, and the middle and right figures show a magnified part of the original image. In the middle and right images, it is clear that there is a strong edge separating  $p_3$  from  $p_1$  and  $p_2$ . expect  $p_1$  to be much more strongly related to  $p_2$  than  $p_3$ . This intuition carries over in definition of dissimilarity between two pixels: if the straight line connecting any two points in an image is separated by a strong edge, they have lower affinity.

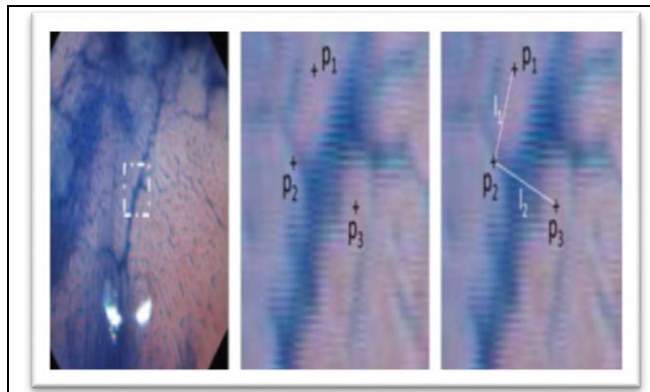


Figure 3: Intervening contours framework.

Analyzing an image (left), three points are chosen for illustration. Pointsp1 andp2 have intuitively higher affinity as compared to any other pair of points.

$$W_{uv} = 1 - \max D$$

D is the diagonal matrix obtained from the various visual features.

5.5. Combining Multiple Visual Features

The optimization process:

$$W = W_{Dce} \times W_{DCr} \times W_{DCo}$$

Where  $W_{Dce}$ ,  $W_{DCr}$  and  $W_{DCo}$  are affinities obtained using edgemaps, creaseness, and color features, respectively. This multiplication of affinities ensures that if one visual feature gives very low similarity between two pixels, the overall similarity between the pixels will be low. Therefore, it automatically caters for the requirement of suppressing the visual features when they are no longer important.

5.6. Normalized Cuts Applied To Image Segmentation Using Visual Features

A graph  $G = (V, E)$  can be partitioned into two disjoint sets A, B. The degree of dissimilarity between these two pieces can be computed as,

$$Cut(A,B) = \sum_{u \in A, v \in B} w(u, v)$$

where  $w(u, v)$  is the similarity between node  $u$  and  $v$ . The optimal bipartitioning of a graph is the one that minimizes this cut value.

This proposed a new measure of disassociation, the normalized cut (NCut):

$$NCut = \frac{cut(A,B)}{assoc(A,V)} + \frac{cut(A,B)}{assoc(B,V)}$$

Where  $assoc(A, V) = \sum_{u \in A, t \in B} w(u, t)$  denotes the total connection from nodes in A to all nodes in the graph and  $assoc(B, V)$  is similarly defined.

Normalized cut criterion is applied to image segmentation by treating each pixel in the image as a point in some arbitrary feature space, represented as a node in the graph. The edge weights between pixel-pairs are specified based on some similarity

between the pixels in terms of the features considered. Segmentation is achieved by partitioning the graph into coherent groups using the NCut criterion. So the grouping algorithm consists of the following steps:

- Given an image, set up a weighted graph  $G = (V, E)$  and set the weight on the edges connecting two nodes being a measure of the similarity between the two nodes using some similarity measure or a set of measures. Form the matrices  $W$  and  $D$ .
- Solve  $(D - W)y = Dy$  for eigenvectors with the smallest eigenvalues.
- Use the eigenvector with second smallest eigenvalue to bi-partition the graph.
- Decide if the current partition should be sub-divided and recursively repartition the segmented parts if necessary. A threshold for NCut could be set so that the recursion stops when the normalized cut value between two partitions at any stage is greater than this threshold.

This method can be used to form  $W$  that can be input to the NCut grouping algorithm to yield hierarchical partitions sequentially.

5.7. Experiments and Results

The performance of proposed segmentation method for segmentation of lesions in GE images that were manually annotated by the physicians. Various visual features are used individually and as their combination to assess the variation in segmentation performance with the use of various visual features from the images.

5.7.1. Segmentation Using A Single Visual Feature

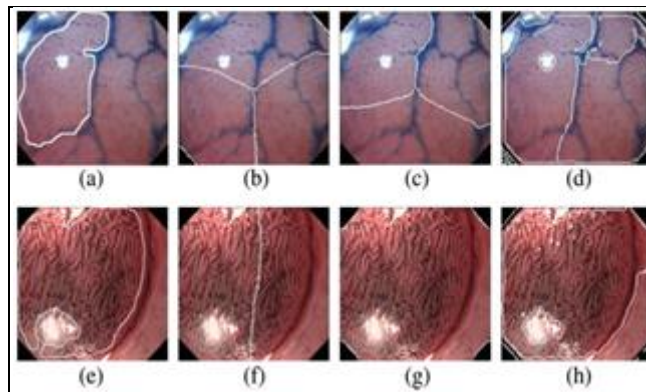


Figure 4: NCut segmentation using different visual features (a) CH Ann. (b) LUV (c) Edgmaps (d) Creaseness. (e) NBI Ann. (f) LUV (g) Edgmaps (h) Creaseness

5.7.2. Segmentation Using a Combined Visual Feature

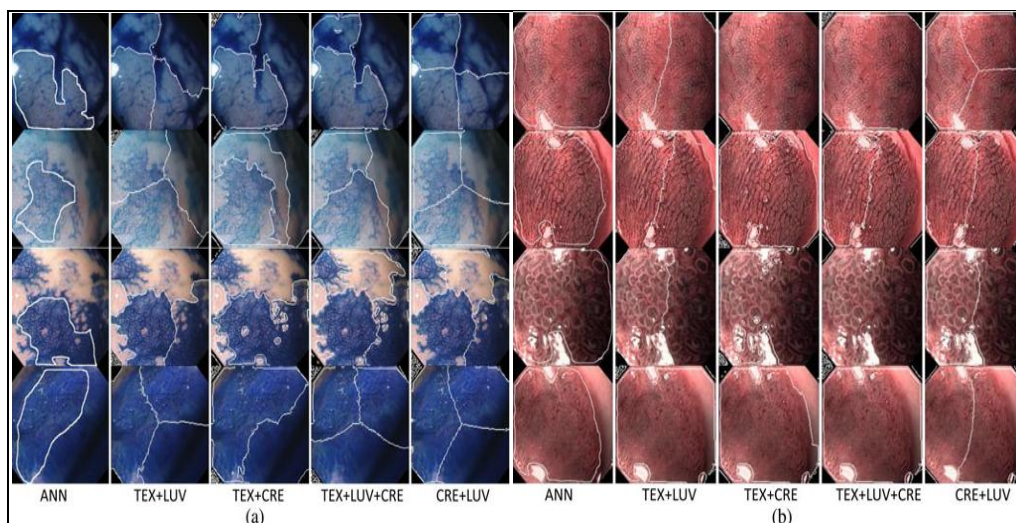


Figure 5: Visual illustration of manual annotations and segmentation obtained using combination of various features (ANN: Annotations; TEX: Edgmaps; LUV: CIELUV color features; CRE: Creaseness). (a) CH images. (b) NBI images.

### 5.9. Comparison Metrics

The quantitative accuracy between the segments obtained by segmentation methods and the manual annotations has been computed using the well-known dice similarity coefficient (DSC) and F-measure. Here represent an annotation as A and an image segment as S, DSC between them can be represented as,

$$DSC = 2 \frac{A \cap S}{A + S}$$

The values of DSC range between 0 and 1 for zero overlap and identical contours, respectively, for annotated and segmented regions. The F-measure between A and P can be represented as,

$$F = 2 \frac{PR}{P+R}$$

Where P is the precision and R is the recall. F-score ranges between 0 and 1 indicating bad or good segmentation, respectively.

	CH		NBI	
	DSC	F	DSC	F
LUV	0.5755	0.5755	0.64	0.64978
TXE	0.64273	0.642	0.75	0.75432
CRE	0.81	0.81181	0.91	0.9149

Table 1: Segmentation results for both GI imaging modalities using single visual features (LUV: color; TEX: Edgemaps; CRE: creaseness; F-Measure; DSC: Dice similarity coefficient)

	NBI		CH	
	DSC	F	DSC	F
TEX+LUV	0.986	0.98677	0.73	0.735
TEX+CRE	0.982	0.98234	0.73	0.735
LUV+CRE	0.985	0.98514	0.81	0.818
TEX+LUV+CRE	0.981	0.9809	0.68	0.688
				2

Table 2: Segmentation results for both GI imaging modalities using combined visual features (Luv: color; Tex: edgemaps; CRE: creaseness; f-measure; DSC: dice similarity coefficient)

## 6. Conclusion

In this context, several gastrointestinal cancer detection techniques have been proposed. In this review these techniques are divided into five major categories: texture, spectral, special, pit pattern, and gene analysis-based techniques. A larger subset of these techniques has been summarized in this paper. Additionally, an extensive comparison of various gastrointestinal cancer detection categories and of multiple techniques within each category has also been provided. Most of the techniques have been implemented in Matlab and tested on unified data set. Analysis reveals that simple texture and Gabor texture analysis-based techniques are better compared to other approaches owing to their ease of use for histopathologists easy access to the equipment, and superior results.

## 7. References

1. S Hwang, M. Areia, F. B. Silva, P. Nunes, M. Dinis-Ribeiro, and M. Coimbra, "Gabor textures for classification of gastroenterology images," in Proc. IEEE Int. Symp. Biomed. Imag., Mar./Apr. 2011, pp. 117–120.
2. M. Mackiewicz, A. Karargyris and N. Bourbakis, "Detection of small bowel polyps and ulcers in wireless capsule endoscopy videos," IEEE Trans. Biomed. Eng., vol. 58, no. 10, pp. 2777–2786, Oct. 2011.
3. Li and Meng, A. Mirko, A. Stefan, and L. Gerard, "Automatic segmentation and inpainting of specular highlights for endoscopic imaging," J. Image Process., vol. 2012, pp. 1–12, 2012.
4. Li and Meng, P. Arbel' aez, C. Fowlkes, and J. Malik, "Contour detection and hierarchical image segmentation," IEEE Trans. Pattern Anal. Mach. Intell., vol. 33, no. 15, pp. 898–916, May 2010.
5. Karkanis, E. Vazquez, R. Baldrich, J. Weijer, "Describing reflectances for color segmentation robust to shadows, highlights, and textures," IEEE Trans. Pattern Anal. Mach. Intell., vol. 33, no. 5, pp. 917–930, May 2011.
6. S. Hwang and M. Celebi, B. Andre, T. Vercauteren, and N. Ayache, "Content-based retrieval in endomicroscopy: Toward an efficient smart atlas for clinical diagnosis," Lecture Notes Comput. Sci., vol. 7075, 2012.
7. A. Karargyris and N. Bourbakis, H. C. Huang, Y. Y. Chuang, and C. S. Chen, "Affinity aggregation for spectral clustering," in Proc. IEEE Conf. Comput. Vis. Pattern Recognit., Jun. 2012, pp. 773–780.
8. C. Demir, Y. Demer Alexandros Karargyris, and Nikolaos Bourbakis, "Detection of Small Bowel Polyps and Ulcers in Wireless Capsule Endoscopy Videos," IEEE Transactions On Biomedical Engineering, Vol. 58, No. 10, October 2011
9. M. Hafner, C. Le Guillou, B. Solaiman, M. Robaszkiewicz, P. LeBeux, and C. Roux, "Computer-assisted diagnosis system in digestive endoscopy," IEEE Trans. Inf. Technol. Biomed., vol. 7, no. 4, pp. 256–262, Dec. 2012.

10. A. Sousa, Olga Veksler, Mena Gaed, José A. Gómez, Madeleine Moussa, Glenn Bauman, "Prostate Histopathology: Learning Tissue Component Histograms for Cancer Detection and Classification," IEEE Transactions On Medical Imaging, Vol. 32, No. 10, October 2013.
11. X. Hu, E. K. Park, and X. Zhang, "Microarray gene cluster identification and annotation through cluster ensemble and EM based informative textual summarization," IEEE Trans. Inf. Technol. Biomed., vol. 13, no. 5, pp. 1–12, Sep. 2010.
12. B. Li and M. Meng, "Computer-aided detection of bleeding regions for capsule endoscopy images," IEEE Trans. Biomed. Eng., vol. 56, no. 4, pp. 1032–1039, Apr. 2012.
13. Y. Fu, M. Mandal, and G. Guo, "Bleeding region detection in wce images based on color features and neural network," in Proc. IEEE 54th Int. Midwest Symp. Circuits Syst., Aug. 2011, pp. 1–4.
14. J. Canny, "A computational approach to edge detection," IEEE Trans. Patt. Anal. Mach. Intell., vol. 8, no. 6, pp. 679–698, Nov. 2010.
15. F. Vilariño, P. Spyridonos, F. De Iorio, J. Vitri` a, F. Azpiroz, and P. Radeva, "Intestinal motility assessment with video capsule endoscopy: Automatic annotation of phasic intestinal contractions," IEEE Trans. Med. Imag., vol. 29, no. 2, pp. 246–259, Feb. 2010.
16. T. F. Chan and L. A. Vese, "Active contours without edges," IEEE Trans. Image Process, vol. 10, no. 2, pp. 266–277, Feb. 2011.